Investigation of Multicomponent Sorption in Polymers from Fluid Mixtures at Supercritical Conditions: The Case of the Carbon Dioxide/Vinylidenefluoride/Poly(vinylidenefluoride) System

Alessandro Galia,* Andrea Cipollina, Onofrio Scialdone, and Giuseppe Filardo

Dipartimento di Ingegneria Chimica dei Processi e dei Materiali, Università di Palermo, Viale delle Scienze, Ed. 6, 90128 Palermo, Italy

Received September 17, 2007; Revised Manuscript Received November 30, 2007

ABSTRACT: The simultaneous sorption of carbon dioxide and vinylidene fluoride (VDF) in poly(vinylidenefluoride) from their supercritical (sc) mixtures was studied using an experimental method, already described in a previous publication, based on the gas-chromatographic determination of the equilibrium composition of the fluid phase in contact with the polymer. Argon was added to the system as a nonabsorbable molecular probe in the polymer to take into account the effect of the volume swelling on the measurement. Sorption behavior has been studied at 50 °C by changing the composition and the density of the supercritical phase. We have found that VDF dissolves in its polymer with concentrations much lower than carbon dioxide at similar total and partial pressures. The mixed fluid CO_2/VDF behaves as a worse solvent toward PVDF with respect to pure CO_2, leading to a reduction of the cumulative sorption. This effect becomes progressively more significant when the fluoromonomer concentration increases. Experimental data obtained from binary systems were fitted using the Sanchez−Lacombe equation of state, and this model was used to estimate the drift in the composition of the polymer phase during the polymerization of VDF in scCO_2. This estimate shows that the concentration of the monomer dissolved in the polymer remains low during the whole polymerization.

1. Introduction

The investigation of sorption of low molecular weight compounds in polymers is a research topic of critical relevance for the validation of models to predict mass uptake and dilation of the material and for several important applications such as the use of polymeric membranes in separation processes, the synthesis and modification of macromolecules in supercritical solvents, and the devolatilization of polymers.

Although many experimental techniques have been proposed to study the sorption of high-pressure gaseous components in polymers, it is difficult to obtain reliable data, since, to decouple the effects of sorption from those of polymer dilation, the latter must be known or measured by a different technique.[1−16] The scenario becomes even more complex when ternary systems are considered since it is necessary to discriminate between the sorption of the different components. In this case, an approach described in the literature for CO_2/polymer/solute systems has been to determine partition coefficients of the solute between the polymer and the supercritical phase by supercritical fluid chromatography[17,18] or by a semistatic experimental technique.[19] In both cases, it was not possible to have simultaneous information on the sorption of the supercritical solvent inside the polymer.

Recently we have described a new gas-chromatographic method that was used to measure the sorption of scCO_2 in poly(vinylidenefluoride) (PVDF) using Ar as a not absorbable molecular probe to take into account the effect of dilation of the macromolecular matrix on the measurements.[20]

In principle, this method can be easily extended to the investigation of multicomponent systems, and we have decided to use it to study the vinylidene fluoride/CO_2/PVDF system.

* Corresponding author. Telephone: +39 091 6567258. Fax: +39 091 6567280. E-mail: galia@dicpm.unipa.it.

PVDF is a thermoplastic semicrystalline polymer having low density, mechanical flexibility, high thermal and oxidative stability, piezo-electricity, and biocompatibility as well as outstanding weatherability.[21] Moreover, the disposition of alternate fluorine and hydrogen atoms leads to unusual polarity within the polymer chains, with a dramatic effect on dielectric properties and solubility. The polymerization of vinylidene fluoride (VDF) has been widely investigated in supercritical carbon dioxide both by precipitation[22−27] and by dispersion[28−31] techniques. Given the heterogeneous character of the polymerization process, two reaction loci may be considered *a priori* and different kinetics and molecular weight distributions can be expected considering the mass transfer kinetics of free radicals among the two phases and the solubility of monomer inside polymer particles. With this premise, the study of the simultaneous sorption of VDF and CO_2 in PVDF is of paramount importance for the rational comprehension of the polymerization and for the proper design of the polymerization strategy. Beside these applicative features, the ternary system CO_2/VDF/PVDF can be considered an interesting model to study the role of crystallinity on multicomponent sorption at high-pressure conditions. In the case of semicrystalline polymers the common adopted approach is ideally to partition the matrix in two parts. The crystalline part is considered impermeable to any species while the amorphous portion is described by a glassy or rubber model depending on the glass transition temperature of the polymer and the operative temperature of the experiments. In the case of PVDF, this simple approach does not seem possible. In fact, Shenoy et al.[32] have observed that the swelling behavior of PVDF at T lower than 100 °C is similar to that observed for glassy polymers such as poly(methylmethacryalte) and poly(styrene) even if measurements were performed at temperatures well above the glass transition temperature of amorphous domains of the fluoropolymer (T_g = −38 °C). Moreover, when experimental data of sorption of scCO_2 in the

10.1021/ma702087s CCC: $40.75
Published on Web 01/19/2008

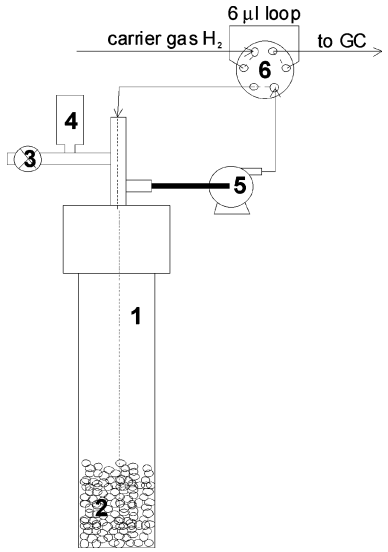

Figure 1. Sketch of the sorption cell and auxiliaries. Key: (1) high-pressure Parr cell; (2) polymer pellets; (3) loading and purging valve; (4) pressure transducer; (5) circulation pump; (6) Rheodyne sampling valve.

polymer were modeled using the Sanchez−Lacombe (S−L) lattice fluid model in predictive form (null interaction parameters in the mixing rules), better results have been obtained using a nonequilibrium version of the equation of state (EOS).[33] Both these observations prompt the consideration that crystalline portions impart to rubbery domains a rigidity that makes their behavior somehow similar to those of glassy regions.

For all these reasons, in the present work, the GC-based technique elsewhere described[20] to measure sorption of $scCO_2$ in PVDF has been extended to investigate the simultaneous sorption of CO_2 and VDF from their mixtures, at different compositions and pressures. Since this study was aimed to obtain thermodynamic information for the mathematical modeling of the polymerization process, experimental data of the binary systems were fitted with the equilibrium versions of the S−L EOS using two-parameter mixing rules. This choice was made because, from the engineering point of view, this version of the EOS was found to give good accuracy when used in nonpredictive manner, fitting interactions parameters from experimental data.[27,31]

2. Experimental Section

2.1. Materials. Poly(vinylidene fluoride) Solef 1010 with melting temperature 173.2 °C, calorimetric crystallinity 55%, $M_n = 120\,600$ and $M_w = 298\,300$ (molecular weight obtained using polystyrene standards) was kindly donated by Solvay Solexis and used in the form of cylindrical pellets (diameter $d = 2$ mm, $d/h = 1$). Prior to the insertion in the sorption vessel the polymer (30 g) was heated to 140 °C for 3 h and then slowly cooled down to room temperature (cooling time 5−7 h). The CO_2 was Air Liquide 99.998 pure, Ar was Air Liquide 5.0, and the VDF monomer was kindly donated by Solvay Solexis (Bollate, Italy). All gases were used without further purification. The carrier gas for the gas chromatographic analyses, carried out with a thermal conductivity detector (TCD), was hydrogen 6.0 produced by a Parker electrolytic gas generator.

2.2. Experimental Apparatus. The experimental apparatus (see Figure 1) consisted of a high-pressure cell Parr model 2670 (1) with a nominal free volume of 72 mL. The cell was fitted with a high precision pressure transducer (4), Sensotec model STJE/1890-20A with accuracy ±0.05 MPa. The mixing in the sorption cell was obtained by a high-pressure magnetically driven gear pump (5), Micropump model GAH−V21-C, with nominal flow rates up to 100 mL/min, thus guaranteeing very short mixing times. The gas mixture was periodically sampled by a six-way Rheodyne valve (6) with a 6 μL loop. Samples were analyzed using a Hewlett-Packard Series HP 6890 gas chromatograph whose carrier circuit was modified to use the hydrogen itself, at 0.6 MPa, to entrain the fluid contained in the sample loop. A Carboxen 1000 chromatographic column was used to separate the components of the gaseous mixture which was analyzed by a TCD.

The high-pressure part of the experimental apparatus (constituted by the sorption vessel, the Rheodyne valve, the body of the circulation pump, and the connections, tubing, and fittings) was inserted as a whole in an electronically controlled oven at a temperature of 50 ± 0.3 °C.

2.3. Experimental Procedure for the Determination of Gas Sorption. Each experiment was performed loading PVDF, Ar, VDF, and CO_2 in the sorption cell and weighing their masses with an electronic balance (accuracy ±0.01 g). Before loading, the system was washed several times with CO_2 at low pressure. Ar was always loaded just after the polymer. In some experiments the noble gas was added using a loading cartridge which allowed a higher precision in estimating the mass (accuracy ±0.002 g). These experiments are characterized by smaller error bars in the experimental data of sorption. After all components were loaded, the sorption cell was inserted in the thermostatic oven and connected to the GC for on-line analysis. The method to determine sorption of a gaseous component in the polymer matrix[20] is based on the solution of the mass balance equation of the soluble component coupled with the conservation equation for the mass of an ideally nonabsorbable molecular probe added to the fluid phase to consider the effect of polymer dilation on the measurement. The extension to a multicomponent system is straightforward, and it consists in the addition of a new mass balance equation for each additional component.

Indeed, in the present investigation, the conceptual simplicity of the method has been put in evidence studying the simultaneous solubility of CO_2 (component 1) and VDF (component 2) in PVDF (component 3) from their binary high-pressure gaseous mixtures. The probe used in this study was the same adopted in our previous investigation, namely Ar, as discussed in a following section. In this case the system of mass balance equations can be summarized as follows:

$$M_i^0 = M_i^P + \rho_i^g(V - V_P^0 - V_P^{Sw}) \quad (1)$$

$$M_{Ar}^0 = \rho_{Ar}^g (V - V_P^0 - V_P^{Sw}) \quad (2)$$

where M_i^0 ($i = 1,2$) and M_{Ar}^0 are the total masses of CO_2, VDF, and argon loaded in the sorption cell, M_i^P are the total amounts of CO_2 ($i = 1$) and VDF ($i = 2$) dissolved in the polymer at equilibrium condition, ρ_i^g are the weight concentrations of the components in the fluid phase at equilibrium, V is the total free volume of the experimental apparatus, V_P^0 is the initial volume of the polymer inserted in the sorption cell and V_P^{Sw} is the volume of swelling of the polymer as a consequence of the sorption of CO_2 and VDF.

From eqs 1−2 we obtain the following expressions for the quantities M_i^P:

$$M_i^P = M_i^0 - \frac{\rho_i^g}{\rho_{Ar}^g} M_{Ar}^0 \quad (3)$$

The density ratio of each component with respect to the probe in the gas phase at equilibrium conditions can be directly measured by gas chromatographic analysis of the sampled gas mixture, while the initial masses of the different components are known. Writing under dimensionless form eq 3, dividing both members by the total mass of the polymer used to perform the experiment (M_P^0), it becomes

$$\frac{M_i^{\mathrm{P}}}{M_{\mathrm{P}}^0} = \frac{M_i^0}{M_{\mathrm{P}}^0} - \frac{\rho_i^{\mathrm{g}}}{\rho_{\mathrm{Ar}}^{\mathrm{g}}} \frac{M_{\mathrm{Ar}}^0}{M_{\mathrm{P}}^0} \tag{4}$$

The mathematical manipulation previously described has been selected because it offers several advantages: it implicitly accounts for the effect of the polymer dilation without the need of computing it; it makes possible to perform GC calibration in terms of mass ratio of the components thus avoiding the necessity of determining the total free volume of the experimental apparatus; it allows the operator to use the not absorbable probe as an internal chromatographic standard to improve the precision of the quantitative analyses as they become unaffected by any density fluctuation in the sampling loop.

The ratio of the density of each soluble component to that of Ar can be expressed in terms of gas chromatographic areas:

$$\frac{\rho_i^{\mathrm{g}}}{\rho_{\mathrm{Ar}}^{\mathrm{g}}} = Y_i = F_i \frac{A_i}{A_{\mathrm{Ar}}} = F_i X_i \tag{5}$$

where X_i are the ratios between the chromatographic areas A_i of each component and that of the probe, A_{Ar}. All of them are related to their mass ratios through the equation of the calibration lines by the response factors F_i. To apply our experimental method, a preliminary calibration of the TCD detector was necessary by preparing gaseous mixtures of CO_2, VDF, and Ar at known composition in the absence of polymer. Calibration points for both components are fairly well fitted by straight lines whose slopes F_i are related to the response factor of each component to the TCD (Figure 2).

Eventually eq 4 can be written as

$$\xi_i = \beta_i - \alpha F_i X_i \tag{6}$$

where ξ_i denotes the mass of absorbed gas per gram of polymer, $\beta_i = M_i^0/M_{\mathrm{P}}^0$ and $\alpha = M_{\mathrm{Ar}}^0/M_{\mathrm{P}}^0$.

2.4. Selection of the Probe. The choice of argon as not-absorbable probe was made on the basis of simple considerations already discussed elsewhere.[20] In fact, Argon has a very low solubility in PVDF (as to allow the assumption of constant mass in the fluid phase) under the conditions adopted in our study, it is completely miscible with CO_2 and VDF and well detectable by the TCD detector using H_2 as a carrier.

Finally, at the low mole fractions used in our experiments, it negligibly affects chemical potentials of the other species in the system, as shown by the plot of the relative deviations in the fugacity of CO_2 and VDF computed as a function of the inert mole fraction at 50 °C and different pressures for fixed weight ratios VDF/CO_2 40/60 (Figure 3) and 20/80 (Figure 4).

In these calculations the fugacities of CO_2 and VDF were estimated using the Peng−Robinson EOS[34] using literature values (Table 1) for the pure component parameters.[35,36] In the van der Waals mixing rule, the interaction parameter between CO_2 and VDF was taken from the literature[36] while null interaction parameters were considered between both components and the noble gas.

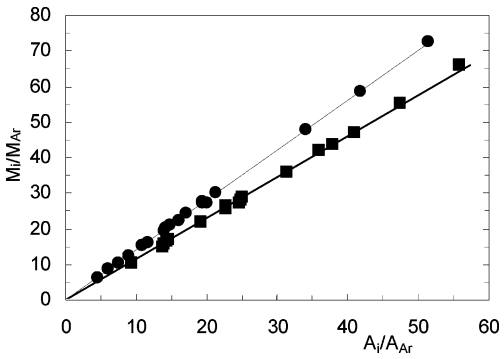

Figure 2. Calibration of the TCD detector for CO_2 (■) and VDF (●) using Ar as internal standard.

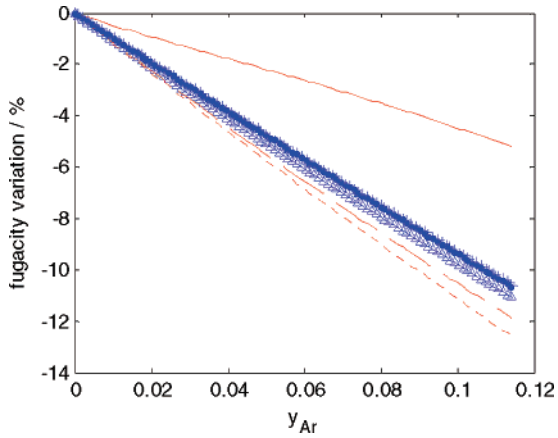

Figure 3. Computed relative variation in the fugacity of CO_2 and VDF (at fixed VDF/CO_2 weight ratio of 40/60) in mixture with Ar as a function of the inert mole fraction at 50 °C and different pressures. CO_2: (blue open triangle) 10 MPa, (blue plus sign) 25 MPa, (blue solid dot) 40 MPa; VDF: (red solid line) 10 MPa, (red dashed line) 25 MPa, (red hyphens) 40 MPa.

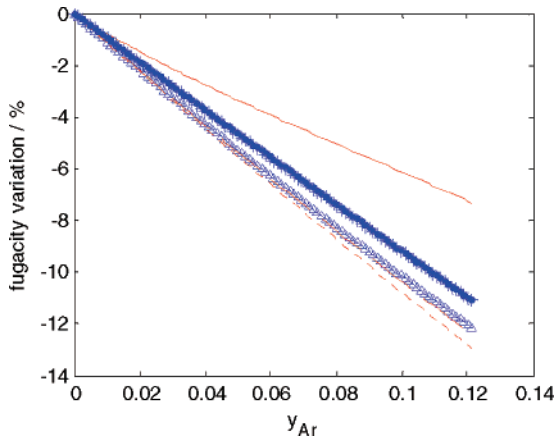

Figure 4. Computed relative variation in the fugacity of CO_2 and VDF (at fixed VDF/CO_2 weight ratio of 20/80) in mixture with Ar as a function of the inert mole fraction at 50 °C and different pressures. CO_2: (blue open triangle) 10 MPa, (blue plus sign) 25 MPa, (blue solid dot) 40 MPa; VDF: (red solid line) 10 MPa, (red dashed line) 25 MPa, (red hyphens) 40 MPa.

Table 1. Pure Component Parameters Used in the PREOS

component	T_c [K]	P_c [MPa]	ω	MW [g mol^{-1}]
CO_2	304.1	7.37	0.225	44.01
VDF	302.8	4.46	0.139	64.03

2.5. Considerations on Mixing Times and Sorption Kinetics. From what was previously reported, it can be easily inferred that the accuracy of the measurements obtained with the present method is strongly dependent on the absence of any gradient in the gas-phase contacted by the polymer at equilibrium conditions. This is particularly important in the case of multicomponent mixtures where unacceptably high levels of segregation in the fluid phase can arise owing to the action of the gravitational field on components of very different molecular weights. For this reason, the mixing of the gaseous phase was improved with respect to previously adopted apparatus using a magnetic driven high-pressure circulation pump that can operate at a maximum nominal flow rate of 100 mL/min. With the adopted configuration of the apparatus it was experimentally observed that high reproducibility in the X_i values of a series of consecutive GC injections was achieved within 2 h of operation of the circulation pump.

Another important parameter that must be estimated for the reliability of the measurements is the time for the achievement of

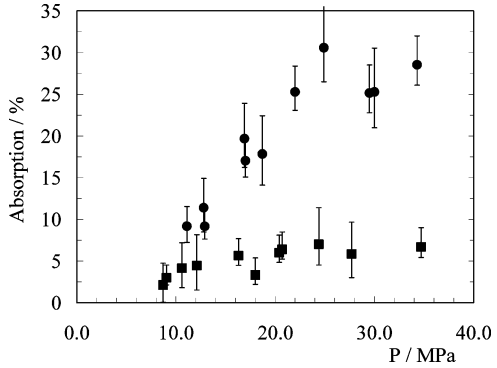

Figure 5. Comparison between solubility of pure components CO_2 (●) and VDF (■) in PVDF as a function of pressure at 50 °C (absorption referred to the mass of amorphous polymer).

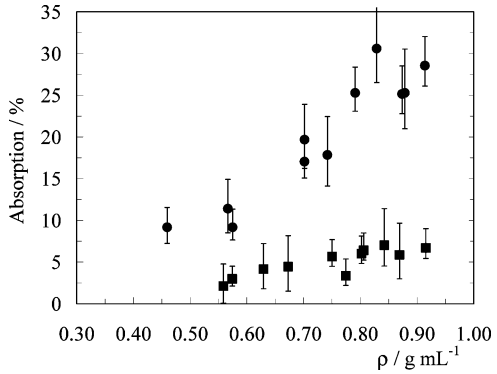

Figure 6. Comparison between solubility of pure components CO_2 (●) and VDF (■) in PVDF as a function of the density of the fluid phase at 50 °C (absorption referred to the mass of amorphous polymer).

equilibrium or pseudo-equilibrium conditions. Such a time was initially estimated approximating each pellet as a sphere of 2 mm of diameter and considering the solution for non-steady diffusion in the particle with constant surface concentration[37] assuming for the diffusion coefficient of CO_2 in PVDF the value of 10^{-7} cm^2/s measured at 4 MPa and 70 °C[38]. With the aforementioned values, a time interval of about 18 h was needed to attain sorption equilibrium. It must be underlined that this value can be considered overestimated since higher CO_2 density should lead to a faster mass transfer rate of the penetrants in the matrix owing to higher swelling of the polymer. Indeed, Briscoe et al.[16] have reported a 1 order of magnitude variation of the diffusion coefficient of CO_2 in PVDF at 80 °C when the pressure changes from 1.5 to 22.5 MPa. To support the hypothesis of fast mass transfer in the pellets we have observed that, when only CO_2 and Ar were loaded in the sorption cell, a stable fluid phase composition, as detected by the GC analyses, was achieved within 12 h from the attainment of thermal equilibrium of the system. Sorption kinetics seemed slower for VDF as about 2 days were required to reach equilibrium.

On these bases, the experimental procedures were designed to load the reactor at the end of the day, thus putting the polymer in contact with the fluid phase overnight with circulation on. By this strategy, the GC analyses were started at least after 12 h from the achievement of thermal equilibrium and they lasted for at least 2 days when VDF sorption was to be determined. With the adopted thermal program each chromatographic run lasted 40 min and at least four consecutive injections were performed to determine the fluid phase composition, thus inherently checking that stable conditions were achieved.

2.6. Main Sources of Experimental Error. The estimation of the uncertainty of the measurements was made using the error analysis of the experimental technique reported elsewhere for the case of sorption of a pure component,[20] its extension to multicomponent systems being quite straightforward. In our technique, we have considered as sources of random errors the uncertainty in the values of the slope F_i of the calibration curves, the imprecision in the values of the ratio X_i of chromatographic areas, the uncertainty in the values of the initially loaded mass of polymer, CO_2, VDF, and probe, all evaluated by electronic scales. A further contribution to the error in the measured quantities can be due to the sorption of the probe inside the polymer matrix that always has the same algebraic sign and leads to an underestimation of the amount of each component dissolved in the polymer. Among all, the uncertainty in the mass of Ar loaded in the reactor and in its sorption in the polymer phase are the most significant. An additional comment must be made on the latter. As it can be considered a systematic error, an overestimation of this term can bias the error, giving the impression that the technique mainly underestimates the sorption. On the basis of this consideration, contrary from what we decided in our previous study, we have not overestimated the sorption of Ar in PVDF with respect to the value that we determined by the Berens method. For this reason, more symmetrical error bars have been used in this study with respect to our previous publication.[20]

3. Experimental Results and Discussion

3.1. Sorption of Pure Components. As a preliminary step to the investigation of the solubility of CO_2 and VDF from their high-pressure binary mixtures in PVDF, the sorption of the two pure compounds was measured to study the effect of the nature of the solute on the values of solubility.

Sorption data of the two compounds are depicted in Figure 5. Solubilities are referred to the mass of amorphous polymer as it is commonly accepted that, in the case of semicrystalline polymers, the absorption of gaseous molecules only occurs in the amorphous domains while crystallites are a nonsorbing nonpermeable phase.[39] For this purpose, polymer samples randomly chosen were analyzed by DSC. Calorimetric measurements were performed on the virgin polymer, on thermally treated PVDF and on specimens obtained after desorption of the dissolved components. By this approach, we have computed a crystallinity of ca. 55% substantially unaffected by the thermal treatment and by the sorption process.

From the comparison of the data, it is evident that the vinyl monomer was found to be significantly less soluble than CO_2 in the polymer. The maximum monomer sorption was about 7 g/(100 g amorphous polymer) and remained substantially constant for pressures higher than 20 MPa. As it is well-known that the solvent power of a supercritical fluid is correlated with its density, the solubilities have been replotted in Figure 6 as a function of the gas-phase densities computed, neglecting the presence of Ar, using the P−R EOS, to rule out the effect of different compressibility among the two fluids. From this graph it is evident that sorption experiments were performed at similar total densities of the two different gaseous components so it seems reasonable to hypothesize that the lower solubility of the monomer in its polymer is to be attributed to weaker interactions between VDF molecules and PVDF segments with respect to what occurs in the case of CO_2.

3.2. Simultaneous Sorption of CO_2 and VDF from Their Mixtures. The polymerization of VDF in $scCO_2$ is an heterogeneous process and two different reaction loci may be considered: the continuous supercritical phase and the dispersed polymer particles. It has been proposed that the relative importance of these two domains in the polymerization kinetics of VDF depends on both thermodynamic and kinetic factors. In this context it could be important to have information on the simultaneous sorption of CO_2 and VDF in PVDF. To our knowledge, no data have been published until now, probably due to the experimental difficulties to perform such measurements.

Table 2. Equilibrium Pressures and Compositions of the Fluid Phase as Detected by GC Analyses

CO_2 (1)−PVDF (3)				VDF (2)−PVDF (3)				CO_2 (1)−VDF (2)−PVDF (3)			
P (MPa)	y_1	y_2	y_{Ar}	P (MPa)	y_1	y_2	y_{Ar}	P (MPa)	y_1	y_2	y_{Ar}
11.1	0.957	0.000	0.043	8.7	0.000	0.948	0.052	11.8	0.643	0.322	0.035
12.8	0.971	0.000	0.029	9.0	0.000	0.966	0.034	19.7	0.651	0.320	0.029
12.9	0.977	0.000	0.023	10.6	0.000	0.954	0.046	18.9	0.677	0.304	0.019
16.9	0.975	0.000	0.025	12.1	0.000	0.963	0.037	20.0	0.651	0.320	0.029
17.0	0.982	0.000	0.018	16.3	0.000	0.975	0.025	24.2	0.652	0.320	0.028
18.7	0.977	0.000	0.023	18.0	0.000	0.976	0.024	27.0	0.638	0.337	0.025
22.0	0.983	0.000	0.017	20.4	0.000	0.977	0.023	31.8	0.668	0.308	0.023
24.9	0.979	0.000	0.021	20.7	0.000	0.966	0.034	34.1	0.677	0.307	0.016
29.5	0.984	0.000	0.016	24.4	0.000	0.964	0.036	36.0	0.668	0.306	0.026
30.0	0.980	0.000	0.020	27.7	0.000	0.962	0.038	14.1	0.820	0.155	0.026
34.3	0.985	0.000	0.015	34.7	0.000	0.978	0.022	19.9	0.822	0.155	0.023
								25.4	0.821	0.154	0.024
								27.0	0.828	0.155	0.016
								28.3	0.825	0.154	0.021
								29.4	0.827	0.150	0.022
								30.5	0.832	0.147	0.021
								32.3	0.850	0.135	0.015
								35.0	0.837	0.145	0.018

As our study was also aimed to investigate the surfactant-assisted polymerization of fluoromonomers in $scCO_2$, we have studied the sorption of the gaseous components at two different VDF compositions chosen within the range occurring in batch polymerizations performed in our lab. Experiments were virtually performed, loading in the system two fluid mixtures with CO_2/VDF initial weight ratios around 60/40 and 80/20. The total pressure of the system was modified changing the total mass of the compressible components. As we are dealing with a ternary system, assuming the effect of the noble gas to be negligible, the equilibrium conditions are fully characterized when three intensive parameters are fixed. All measurements were performed at the same temperature usually adopted in polymerization experiments ($T = 50$ °C) so that 2 degrees of freedom remain to be defined. These are the total pressure of the system and the mole fraction of one of the two components at equilibrium conditions.

In the current setup of the experimental apparatus, it is not possible to perform the experiments at fixed equilibrium composition of the fluid phase. We have in any case observed that, in the investigated system, by fixing the initial mass ratio of the soluble components it is possible to obtain systems with almost constant fluid phase composition. This can be verified by comparing data of equilibrium compositions in Table 2, determined by GC analyses.

On the basis of this consideration, we have plotted experimental data in two dimensions, defining the curves as a function of the initial composition of the fluid phase. In Figures 7 and 8, experimental sorption data of CO_2 and VDF, respectively, are plotted as a function of the total pressure at equilibrium. Both compounds exhibit a symmetrical behavior since the amount of each component dissolved in the polymer at fixed P decreases when its concentration in the fluid phase is depleted. Under the adopted conditions the fluoromonomer was much less soluble in the polymer than carbon dioxide reaching a maximum concentration of about 3.7 g per 100 g of amorphous polymer at 36.0 MPa and 0.320 ± 0.016 mole fraction in the supercritical phase.

From the study of the solubility of the pure components, it can be observed that VDF is a poorer solvent for PVDF than CO_2. Hence the behavior of the mixtures could be explained by hypothesizing that when the sc phase is diluted with VDF the number of PVDF−CO_2 donor (−F) acceptor (CO_2) interactions decreases, being replaced by less effective VDF−PVDF interactions. On this basis, the cumulative concentration of the components in the polymer phase should be expected to diminish when VDF replace CO_2 in the mixture. Indeed when sorption values obtained with pure CO_2 are compared with those measured in the presence of VDF, we have found that the total amount of dissolved compounds decreases when the VDF concentration in the gas phase increases (Figure 9). This should lead to lower swelling of the polymer with respect to what happens in pure carbon dioxide and is similar to what is observed for the solubility of liquid solvents in cross-linked or semicrystalline polymers whose swelling decreases when the difference between cohesion parameters of the two species increases.[40]

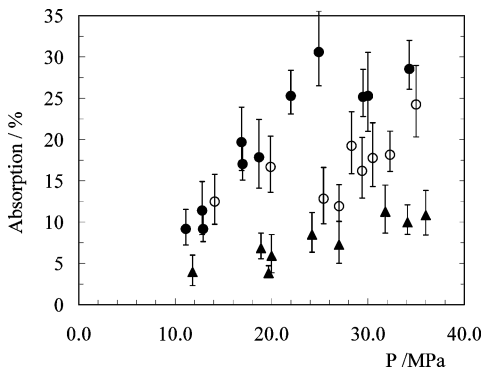

Figure 7. Sorption of CO_2 in PVDF as a function of the total pressure at 50 °C: (●) pure CO_2; (○) CO_2/VDF mixture with initial composition 80/20 w/w; (▲) CO_2/VDF mixture with initial composition 60/40 w/w (solubility referred to the mass of amorphous polymer).

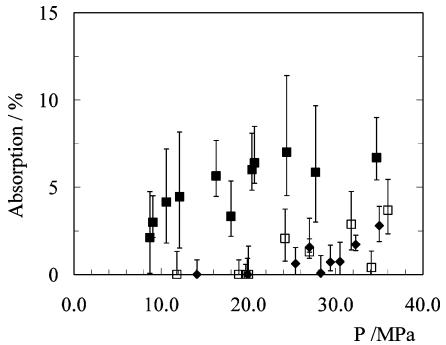

Figure 8. Sorption of VDF in PVDF as a function of the total pressure at 50 °C: (■) pure VDF; (□) CO_2/VDF mixture with initial composition 60/40 w/w; (◆) CO_2/VDF mixture with initial composition 80/20 w/w (solubility referred to the mass of amorphous polymer).

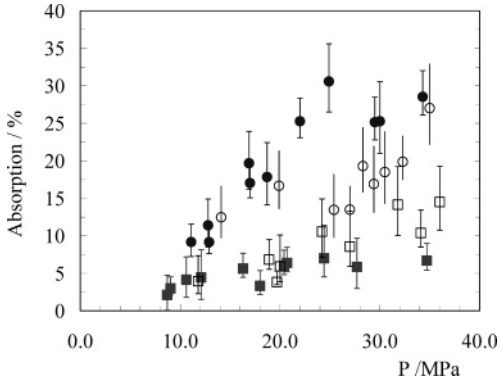

Figure 9. Cumulative sorption of CO_2 and VDF in PVDF as a function of the total pressure at 50 °C: (●) pure CO_2; (○) CO_2/VDF mixture with initial composition 80/20 w/w; (□) CO_2/VDF mixture with initial composition 60/40 w/w; (■) pure VDF (solubility referred to the mass of amorphous polymer).

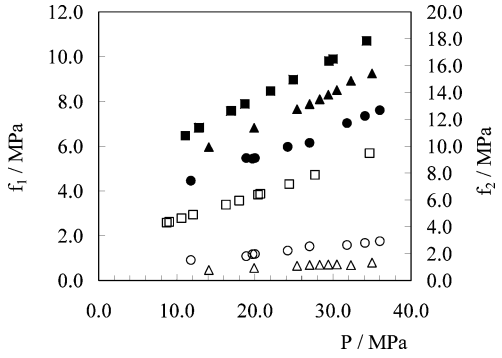

Figure 10. Estimated fugacities of CO_2 (filled symbols) and VDF (open symbols) as a function of total pressure computed at 50 °C from data reported in Table 1. Key: (■, □) pure compounds; (●, ○) CO_2/VDF mixture with initial composition 60/40 w/w; (▲, △) CO_2/VDF mixture with initial composition 80/20 w/w.

Since the quantitative description of the equilibrium distribution of a generic component *i* among all the phases present can be expressed in term of fugacities, it could be interesting to compare sorption in term of this auxiliary function. Fugacities were calculated at 50 °C using the Peng−Robinson EOS with van der Waals mixing rules, taking from the literature binary interaction parameters,[36] and have been plotted in Figure 10 as a function of the total pressure. We have found that while the fugacity of CO_2 f_1 increases with P in all investigated systems, the fugacity of VDF f_2 is much less affected by the total pressure in the binary systems, being roughly constant in the mixture with the highest CO_2 content.

Solubility of CO_2 and VDF are plotted as a function of the fugacity of each component in the mixture. In the case of carbon dioxide (Figure 11), sorption values seem to have a tendency to merge in a single master curve when they are represented as a function of f_1. Differently, in the case of VDF sorption, it seems that even if its mole fraction in the mixture is decreased, the amount of fluoromonomer dissolved in the polymer at the same fugacity increases (Figure 12). This behavior could be attributed to a cosolvent effect toward dissolution of VDF inside the polymer played by carbon dioxide.

4. Considerations on the Heterogeneous Polymerization of VDF in scCO₂

The experimental data obtained studying the ternary system were used to estimate the drift of the monomer concentration in the fluid and polymer phase during the heterogeneous polymerization of VDF in $scCO_2$. This issue could be useful to

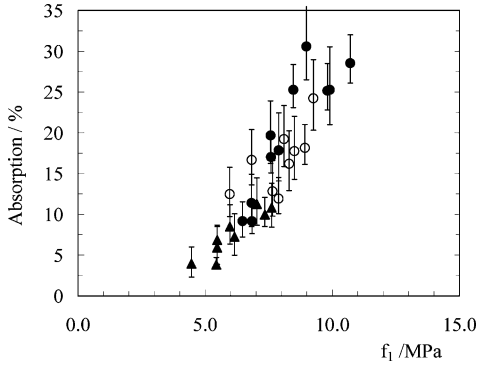

Figure 11. Sorption of CO_2 in PVDF as a function of its fugacity f_1 at 50 °C: (●) pure CO_2; (○) CO_2/VDF mixture with initial composition 80/20 w/w; (▲) CO_2/VDF mixture with initial composition 60/40 w/w (solubility referred to the mass of amorphous polymer).

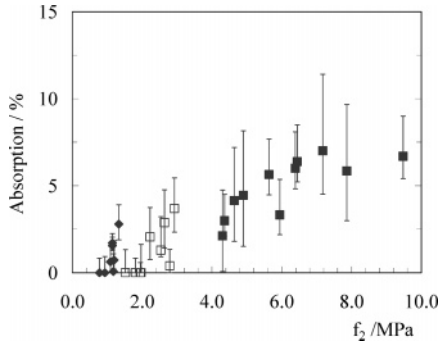

Figure 12. Sorption of VDF in PVDF as a function of its fugacity f_2 at 50 °C: (■) pure VDF; (□) CO_2/VDF mixture with initial composition 60/40 w/w; (◆) CO_2/VDF mixture with initial composition 80/20 w/w (solubility referred to the mass of amorphous polymer).

make clearer the role of each of the two different phases as a polymerization locus. In fact, even if the synthesis of PVDF in $scCO_2$ has been object of several investigations, as already indicated in the introduction of this work, there is still an open discussion on the main site of polymerization.

To this purpose, we can write the mass balance equations for VDF and CO_2 in the case of a batch polymerization, considering that the initial amount of monomer is partially converted to polymer and that both components are partitioned between the fluid phase and the amorphous portions of the polymer phase:

$$M_2^0 = [1 + \xi_2(1 - X_c)]XM_2^0 + M_2^f \quad (7)$$

$$M_1^0 = \xi_1(1 - X_c)XM_2^0 + M_1^f \quad (8)$$

where M_i^0 are the initial masses of VDF ($i = 2$) and CO_2 ($i = 1$) loaded in the reactor, X is the monomer conversion, ξ_i are the amounts of VDF and CO_2 dissolved in the polymer (expressed in grams per gram of amorphous polymer), X_c is the polymer crystallinity and M_i^f are the masses of VDF and CO_2 in the fluid phase at X monomer conversion.

To estimate the drift in the monomer concentration during the polymer synthesis we have used the polymerization recipe and the conversion and pressure profiles obtained when we have studied the kinetics of the polymerization of VDF in the presence of perfluoropolyether stabilizers.[31]

To close the algebraic system, we need a quantitative expression of the sorption terms ξ_i in eqs 7 and 8. This requires a mathematical model to estimate sorption at conditions different from those experimentally investigated.

The theoretical modeling of sorption of gaseous molecules in polymers is a topic of relevant interest both for applications and for theoretical aspects. Models developed so far vary from the simple Henry's law, which can be usefully applied to gas−polymer melt solutions at low pressures, to more complex equations of state based approaches, which take into account several additional aspects, thus guaranteeing a better predictive behavior also for systems at higher pressures. The scenario becomes even more complex if a semicrystalline polymer is considered, as crystalline domains are rigid portions that decrease the mobility of the chains in amorphous domains and cause an elastic retractive force that is opposed to the sorption of the solvent in the polymer. For these materials, it has been proposed that the swelling can be expressed as a sum of a mixing and elastic contribution similar to what is done for cross-linked macromolecules. Thus, the free energy change can be expressed by the following equation

$$\Delta G_{\text{swell}} = \Delta G_{\text{mix}} + \Delta G_{\text{el}} \tag{9}$$

in this equation ΔG_{mix} takes into account the polymer−solvent interactions while ΔG_{el} incorporates the constraining effect of the crystalline junction. On the basis of these considerations, nonequilibrium models also have been used to model sorption data of CO_2 in PVDF. Since the aim of this study was just to obtain an estimate of the monomer concentration in the two different phases in view of the synthesis of PVDF in $scCO_2$, we have used an approach based on the Sanchez−Lacombe EOS to fit pure component sorption data and use the interaction parameters obtained in this way to compare prediction of this model with the behavior observed in the experimental investigation of ternary systems.

This EOS was selected because it has been already used to describe the thermodynamics of low molecular weight species in the mathematical modeling of heterogeneous polymerization of VDF in $scCO_2$.[27,31]

The molecular lattice fluid theory developed by Sanchez and Lacombe[41] is formally similar to the Flory−Huggins theory. In the case of a mixture, each component is divided into mers that are placed into a lattice and allowed to interact with a mean-field intermolecular potential. The crucial difference among the two theories is that the SL model includes empty lattice sites so that volume changes upon mixing can be taken into account. The resulting EOS is presented in terms of dimensionless reduced variables, namely reduced pressure $\tilde{P}$, reduced temperature $\tilde{T}$, and reduced density $\tilde{\rho}$ of the mixture:

$$\tilde{P} + \tilde{\rho}^2 + \tilde{T}\left[\ln(1-\tilde{\rho}) + \left(1 - \frac{1}{r}\right)\tilde{\rho}\right] = 0 \tag{10}$$

The reduced variables in eq 10 are defined in terms of lattice dependent characteristic density (ρ^*), pressure (P^*), and temperature (T^*) of the mixture that, in turn, are functions of v^*, ϵ^*, and r that are, respectively, the close-packed molar volume of a mer corresponding to the volume of 1 mol of lattice sites, the interaction energy per mer, and the number of lattice sites occupied by a molecule of the mixture with molar mass M:

$$\tilde{\rho} = \frac{\rho}{\rho^*} = \frac{rv^*}{Mv}$$

$$\tilde{P} = \frac{P}{P^*} = \frac{Pv^*}{\epsilon^*}$$

$$\tilde{T} = \frac{T}{T^*} = \frac{RT}{\epsilon^*}$$

In the case of a mixture, appropriate mixing rules are necessary to calculate characteristic parameters starting from those of pure components that are usually evaluated by fitting experimental data of some suitable thermodynamic property of the pure component. In this study, mixing rules with two adjustable parameters proposed by McHugh and Krukonis[42] were used:

$$v^* = \sum_i \sum_j \phi_i \phi_j v_{ij}^*$$

with

$$v_{ij}^* = \frac{v_{ii}^* + v_{jj}^*}{2}(1 - \eta_{ij})$$

where η_{ij} is an adjustable parameter used to take into account deviations from the arithmetic mean of v^*_{ij}. The volume fraction of component ith (ratio between the number of sites occupied by component i and total number of lattice sites) is defined as

$$\phi_i = \frac{\omega_i / v_i^* \rho_i^*}{\sum_i (\omega_i / v_i^* \rho_i^*)} \tag{11}$$

where ω_i is the mass fraction of component i in the mixture and ρ_i^* and v_i^* are, respectively, the characteristic mass density and close-packed molar volume of component i.

The mixing rule for the characteristic interaction energy for the mixture ϵ^* is given by

$$\epsilon_{\text{mix}}^* = \frac{1}{v_{\text{mix}}^*} \sum_i \sum_j \phi_i \phi_j \epsilon_{ij}^* v_{ij}^* \tag{12}$$

with

$$\epsilon_{ij}^* = (\epsilon_{ii}^* \cdot \epsilon_{jj}^*)^{0.5} \cdot (1 - \zeta_{ij}) \tag{13}$$

where ζ_{ij} is a second adjustable parameter, used to correct the geometric mean, accounting for specific binary interactions between the species i and j.

As regards the number of lattice sites occupied by a molecule of ith component in the mixture (r_i), it is assumed that this parameter does not change with respect to the value for the pure component:

$$r_i = r_i^{\circ} \tag{14}$$

while the mixing rule used to calculate r is

$$\frac{1}{r} = \sum_i \frac{\phi_i}{r_i} \tag{15}$$

According to SL theory, the chemical potential for the ith component can be calculated by the following equation:

$$\frac{\mu_i}{RT} = \ln(\phi_i) + \left(1 - \frac{r_i}{r}\right) - \frac{\tilde{\rho} r_i \left[\frac{2}{\nu^*}(X_i - \epsilon^* Y_i) + \epsilon^*\right]}{RT} + r_i \left[\left(\frac{1}{\tilde{\rho}} - 1\right)\ln(1-\tilde{\rho}) + \frac{\ln(\tilde{\rho})}{r_i} + \frac{P}{\tilde{\rho}}\frac{(2Y_i - \nu^*)}{RT}\right] \tag{16}$$

where

$$X_i = \sum_j \phi_j v_{ij}^* \epsilon_{ij}^* \tag{17}$$

$$Y_i = \sum_j \phi_j v_{ij}^* \tag{18}$$

Equilibrium partitioning of VDF and CO_2 can be evaluated by equating chemical potentials of each component in the fluid phase and in the polymer phase. In these calculations, the crystalline part of the polymer was assumed to be impermeable to all species and for this reason was not considered in the phase equilibria computation. This means that the volume of the polymer phase used in all calculations is just constituted by the amorphous part of the total polymer volume V_a that was computed on the basis of the crystal fraction X_c:

$$V_a = (1 - X_c)V_p \tag{19}$$

The crystal fraction of PVDF used in sorption experiments was estimated by calorimetric measurements on polymer samples randomly obtained from the virgin material, from the thermally treated polymer and on specimens obtained after CO_2 desorption. A crystallinity of ca. 55%, substantially unaffected both by the thermal treatment than by the sorption process, was determined.

The pure parameters for PVDF were taken from the literature[43] while those for gaseous compounds were fitted to experimental density data at 50 °C taken from NIST database (CO_2) or obtained by loading a fixed volume vessel with different masses of the fluoromonomer and recording P vs T profiles. All the values of the characteristic parameters are summarized in Table 3.

Binary interaction parameters ζ_{ij} and η_{ij} were fitted by a least-square method to experimental density data for the fluid mixture VDF−CO_2 (Figure 13) and to experimental sorption data for the binary systems CO_2−PVDF and VDF−PVDF (Figure 14). The optimized values of the interactions parameters are summarized in Table 4. In the case of the binary systems PVDF−CO_2 and PVDF−VDF, the best fitting of experimental sorption data was obtained taking null interaction parameters for the closed packed volumes. When sorption of CO_2 was considered, as already observed by Kennedy et al.,[44] we found that the S−L model overpredicts and underpredicts sorption data respectively at low and high pressures. A similar behavior was found also in the case of the sorption of pure VDF, but in this case, the quantitative agreement between the model and the experiments is much better.

The S−L model, with interaction parameters regressed from experimental data of binary systems, has been used to predict sorption data in the case of the ternary system at experimentally determined T, P, and average composition of the fluid phase at equilibrium. Comparison between the calculated and experimentally determined sorption data are highlighted in Figures 15 and 16.

Table 3. Values for the S−L Pure Component Parameters for CO_2, VDF and PVDF

	ρ^* [g/cm^3]	v^* [cm^3/mol]	ϵ^* [J/mol]
CO_2	1.450	5.806	2728
VDF	1.065	28.42	3602
PVDF	1.723	12.63	5767

Table 4. Optimized Values for the Binary Interactions Parameters of the System CO_2 (1), VDF (2), and PVDF (3)

ζ_{12}	ζ_{13}	ζ_{23}	η_{12}	η_{13}	η_{23}
0.120	0.032	0.110	0.240	0.000	0.000

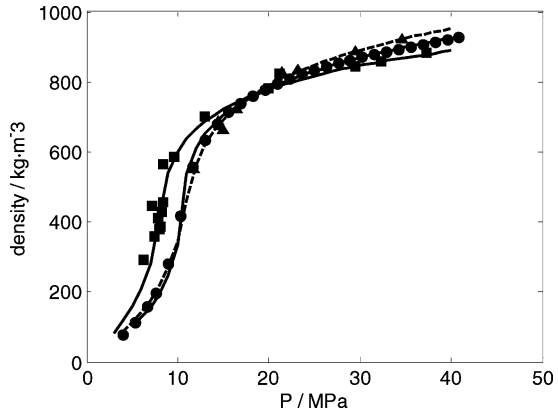

Figure 13. Density of pure CO_2 (●), VDF (■), and CO_2/VDF (▲) mixtures with composition 63/37 w/w as a function of total pressure at $T = 50$ °C. Comparison was made between S−L predictions and experimental data, after fitting binary interaction parameters.

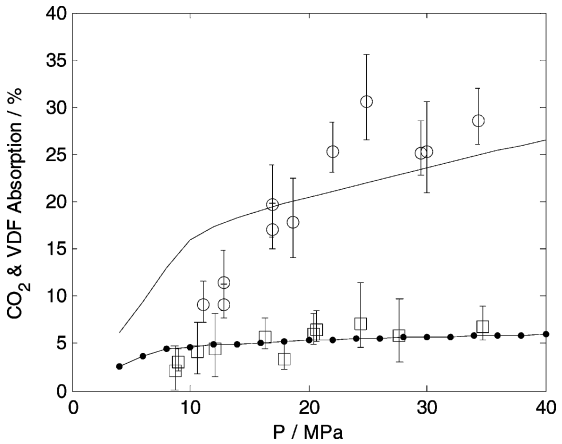

Figure 14. Fitting of experimental sorption data of pure CO_2 (○) and VDF (□) in PVDF at $T = 50$ °C using the SL−EOS model. Sorption expressed in terms of g/100 g of amorphous polymer.

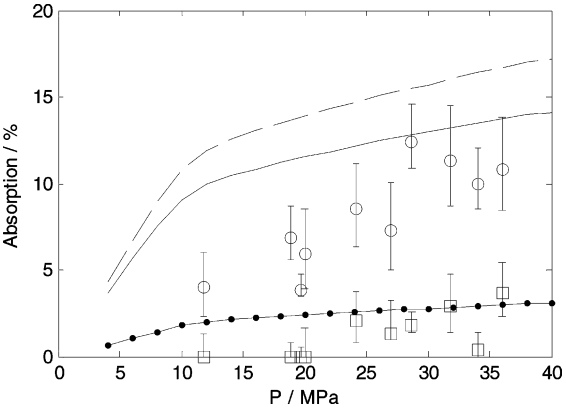

Figure 15. Comparison of SL model predictions with experimental data for mixtures CO_2/VDF (60/40 w/w). $T = 50$ °C. Experiments: CO_2 (○) and VDF (□). S−L predictions: (− − −) total absorption, (—) CO_2, (−•−•−) VDF. Sorption expressed in terms of g/100 g of amorphous polymer.

The qualitative trend of the sorption data is substantially described by the calculated curves. Quite interestingly, simply on the basis of the behavior of the pure components, the adopted thermodynamic model is able to predict the low sorption data of the fluoromonomer in its polymer. The quantitative agreement between the predictions of the model and the experimental data is limited in the case of the CO_2 while a better match between calculated and experimentally determined values was found once more in the case of VDF. On this basis, we can conclude that

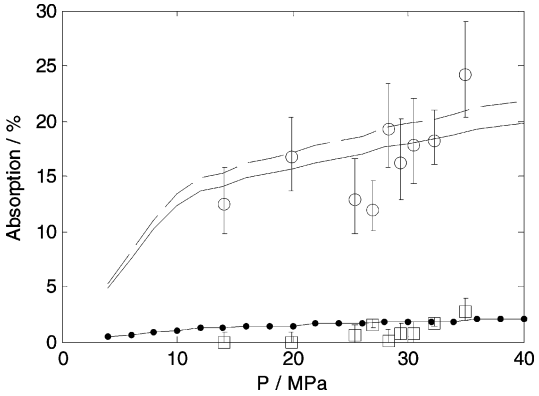

Figure 16. Comparison of SL model predictions with experimental data for mixtures CO_2/VDF (80/20 w/w). $T = 50$ °C. Experiments: CO_2 (○) and VDF (□). S−L predictions: (− − −) total absorption, (—) CO_2, (−•−•−) VDF. Sorption expressed in terms of g/100 g of amorphous polymer.

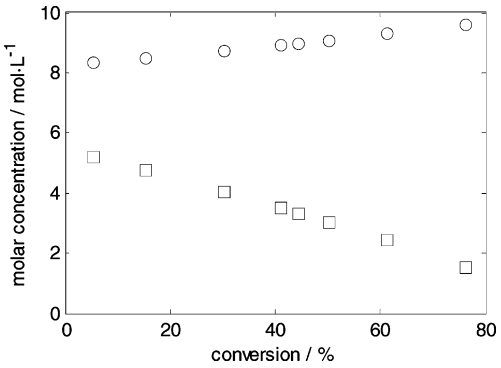

Figure 17. Estimated drift in the molar concentration of VDF (□) and CO_2 (○) in the fluid phase as a function of monomer conversion during VDF polymerization.

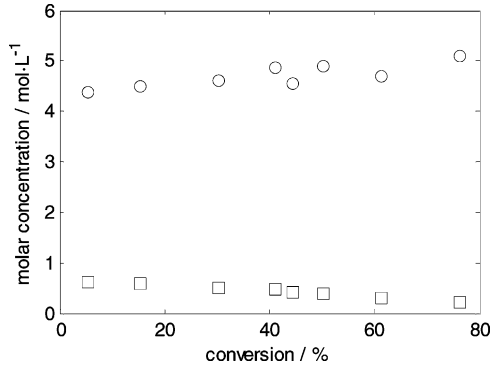

Figure 18. Estimated drift in the molar concentration of VDF (□) and CO_2 (○)in the polymer phase as a function of monomer conversion during VDF polymerization.

the adopted approach is accurate enough to have an estimation of the drift of monomer concentration in the fluid and polymer phase under operative conditions occurring during polymerization of VDF.

The concentration profiles of VDF and CO_2 in the supercritical and polymer phase are plotted in Figures 17 and 18 respectively. In these calculations an average value of crystallinity of 0.65 was used as obtained by DSC analyses of as-polymerized PVDF.[30] The polymerization recipe and the conversion profile used for the calculations have been reported elsewhere.[31] In the fluid phase, the monomer concentration markedly decreases while the polymerization proceeds. The CO_2 density increases with conversion reasonably as a consequence of the excluded volume effect of the synthesized polymer. The molar concentration of VDF inside the polymer is much lower than that in the fluid even if it decreases in a more gradual manner during the polymerization, ranging between about 0.58 and 0.29 M when monomer conversion changes from 4 to 76% at 38 MPa initial pressure and 5.5 M initial concentration of VDF. The more gradual variation of concentration in the polymer phase compared with its steeper decrease in the fluid phase is an alternative manifestation of the aforementioned enhancement in the solubility of VDF in the polymer when the gas phase is enriched in carbon dioxide.

In the case of the polymerization of VDF in $scCO_2$, there is still uncertainty on the main site of the polymerization as, given the low solubility of PVDF in the supercritical solvent, two reaction loci can be considered *a priori*: the CO_2-rich continuous phase and the polymer-rich dispersed phase. On the basis of experiments performed in a continuous stirred tank reactor based reaction system, a mathematical model based on the hypothesis that the main locus of polymerization is the continuous phase was proposed.[23] The model gave good predictions of the polymerization rate but it was not able to predict the bimodal molecular weight distribution exhibited by the polymer when its synthesis is carried out with inlet monomer concentrations higher than 1.7 M.[24] This model was later modified to account qualitatively for the bimodality of MWDs of the polymer by postulating a variation of the termination rate constant with the chain length owing to a decrease in the mobility of growing macroradicals when their size exceeds a critical chain length.[45]

An alternative explanation of the bimodality was proposed by Muller et al.[27] considering that the low molecular weight mode arises from macroradicals terminated in the continuous phase while the high molecular weight peak is constituted by chains terminated in the polymer phase. These authors have proposed that the relative amounts of the two modes depend on the rate of interphase transport of radical chains. To support this hypothesis, it was observed that when the polymerization is carried out in the presence of an effective stabilizer leading to the formation of a dispersed phase with high interfacial area, the bimodality is suppressed and only the high molecular weight mode is observed[31] since macroradicals initiated in the continuous phase may be promptly captured by polymer particles and grow in a locally high viscous medium where the termination is impeded.

Even if sorption data collected in this study do not allow a net discrimination between the two possibilities, in our opinion they supply a useful piece of information in the discussion of the kinetics of the polymerization of VDF in $scCO_2$. As previously underlined we have found that the monomer concentration in the amorphous polymer is rather low at polymerization conditions. This suggests that macroradicals initiated or captured in the polymer phase propagate under starved conditions that could partially compensate the autoacceleration effect arising from the impeded termination.

To support these considerations, when we have performed precipitation and dispersion polymerizations under similar operative conditions, we have observed[30] a much more limited variation in the polymer yield (from 44 to 65%) with respect to what observed for example in the case of the polymerization of methyl methacrylate that should have a significantly higher solubility in its polymer.[46]

On this basis, one could postulate a limited enhancement of the polymerization rate when the main locus of polymerization shifts from the continuous to the particle phase, and this could be a possible explanation for the fact that an homogeneous model can satisfactorily predict the polymerization rate.

5. Conclusions

The sorption of CO_2 and VDF in poly(vinylidenefluoride) was studied using an experimental apparatus based on the utilization of a gas-chromatograph to determine the equilibrium composition of the fluid phase contacted by the polymer and using argon as a nonabsorbable molecular probe to consider the effect of the volume swelling on the measurement.

Sorption behavior was studied at 50 °C both for the pure compounds and for their mixtures changing the composition and the density of the supercritical phase. VDF was found significantly less soluble than CO_2 at similar total and partial pressure, with a maximum sorption, in the case of pure VDF, of about 7 g/(100 g of amorphous polymer), which remained substantially constant for pressures higher than 20 MPa.

If sorption data are plotted as a function of the fugacity of the compounds, it seems that CO_2 dissolved in the polymer has a cosolvent effect toward the fluoromonomer.

Experimental data obtained from binary systems were fitted using the Sanchez−Lacombe equation of state and this model was used to estimate the drift in the composition of the polymer phase during the polymerization of VDF in $scCO_2$. From collected experimental results, we have found that the concentration of the monomer dissolved in the polymer maintains roughly constant at a rather low value during the whole polymerization. This suggests that macroradicals initiated or captured in the polymer phase propagate under starved conditions that could partially compensate for the autoacceleration effect arising from the impeded termination, thus reducing differences in the polymerization rate that should accompany the shift of the locus of polymerization from the continuous to the polymer phase.

Acknowledgment. The financial support of EU (Growth Program ECOPOL, Project Contract No. G1RDCT-2002-00676) of the Università di Palermo and of MIUR is gratefully acknowledged.

References and Notes

(1) Stern, S. A.; De Meringo, A. H. *J. Polym. Sci., Polym. Phys. Ed.* **1978**, *16*, 735−751.
(2) Sato, Y.; Yurugi, M.; Fujiwara, K.; Takishima, S.; Masuoka, H. *Fluid Phase Equilib.* **1996**, *125*, 129−138.
(3) Sato, Y.; Fujiwara, K.; Takikawa, T.; Sumarno; Takishima, S.; Masuoka, H. *Fluid Phase Equilib.* **1999**, *162*, 261−276.
(4) Wissinger, R. G.; Paulatis, M. E. *J. Polym. Sci., Part B: Polym. Phys.* **1987**, *25*, 2497−2510.
(5) Chang, S. H.; Park, S. C.; Shim, J. J. *J. Supercrit. Fluids* **1998**, *13*, 113−119.
(6) Kamiya, Y.; Hirose, T.; Mizoguchi, K.; Naito, Y. *J. Polym. Sci., Part B: Polym. Phys.* **1986**, *24*, 1525−1539.
(7) Kikic, I.; Lora, M.; Cortesi, A.; Sist, P. *Fluid Phase Equilib.* **1999**, *158*−*160*, 913−921.
(8) Kleinrahm, R.; Wagner, W. *J. Chem. Thermodyn.* **1986**, *18*, 739.
(9) Von Schnitzler, J.; Eggers, R. *J. Supercrit. Fluids.* **1999**, *16*, 81−92.
(10) Sato, Y.; Takikawa, T.; Takishima, S.; Masuoka, H. *J. Supercrit. Fluids* **2001**, *19*, 187−198.
(11) Sato, Y.; Takikawa, T.; Yamane, M.; Takishima, S.; Masuoka, H. *Fluid Phase Equilib.* **2002**, *194*−*197*, 847−858.
(12) Rajendran, A.; Bonavoglia, B.; Forrer, N.; Storti, G.; Mazzotti, M.; Morbidelli, M. *Ind. Eng. Chem. Res.* **2005**, *44*, 2549−2560.
(13) Bonner, D. C.; Cheng, Y. J. *J. Polym. Sci., Polym. Lett. Ed.* **1975**, *13*, 259−264.
(14) Aubert, J. H. *J. Supercrit. Fluids.* **1998**, *11*, 163−172.
(15) Briscoe, B. J.; Mahgerefteh, H. *J. Phys. E: Sci. Instrum.* **1984**, *17*, 483−487.
(16) Briscoe, B. J.; Lorge, O.; Wajs, A.; Dang, P. *J. Polym. Sci., Part B: Polym. Phys.* **1998**, *36*, 2435−2447.
(17) Shim, J. J.; Johnston, K. P. *AIChE J.* **1989**, *35*, 1097−1106.
(18) Inomata, H.; Honma, Y.; Imahori, M.; Arai, K. *Fluid Phase Equilib.* **1999**, *158*−*160*, 857−867.
(19) Wu, J.; Pan, Q.; Rempel, G. L. *J. Appl. Polym. Sci.* **2002**, *85*, 1938−1944.
(20) Galia, A.; Abduljawad, M.; Scialdone, O.; Filardo, G. *AIChE J.* **2006**, *52*, 2243−2253.
(21) Carlson, D. P.; Schmiegel, W. In *Ullmann's Encyclopedia of Industrial Chemistry Release 2004*, 7th ed.; Wiley-VCH Verlag GmbH & Co. KGaA: Weinheim, Germany, 2004; DOI: 10.1002/14356007.a11_393.
(22) Charpentier, P. A.; Kennedy, K. A.; DeSimone, J. M.; Roberts, G. W. *Macromolecules* **1999**, *32*, 5973−5975.
(23) Charpentier, P. A.; DeSimone, J. M.; Roberts, G. W. *Ind. Eng. Chem. Res.* **2000**, *39*, 4588−4596.
(24) Saraf, M. K.; Gerard, S.; Wojcinski, L. M., II; Charpentier, P. A.; DeSimone, J. M.; Roberts, G. W. *Macromolecules* **2002**, *35*, 7976−7985.
(25) Galia, A.; Caputo, G.; Spadaro, G.; Filardo, G. *Ind. Eng. Chem. Res.* **2002**, *41*, 5934−5940.
(26) Tai, H.; Liu, J.; Howdle, S. M. *Eur. Polym. J.* **2005**, *41*, 2544−2551.
(27) Mueller, P. A.; Storti, G.; Morbidelli, M.; Apostolo, M.; Martin, R. *Macromolecules* **2005**, *38*, 7150−7163.
(28) Tai, H.; Wang, W.; Martin, R.; Liu, J.; Lester, E.; Licence, P.; Woods, H. M.; Howdle, S. M. *Macromolecules* **2005**, *38*, 355−363.
(29) Tai, H.; Wang, W.; Howdle, S. M. *Macromolecules* **2005**, *38*, 1542−1545.
(30) Galia, A.; Giaconia, A.; Scialdone, O.; Apostolo, M.; Filardo, G. *J. Polym. Sci., Part A: Polym. Chem.* **2006**, *44*, 2406−2418.
(31) Mueller, P. A.; Storti, G.; Morbidelli, M.; Costa, I.; Galia, A.; Scialdone, O.; Filardo, G. *Macromolecules* **2006**, *39*, 6483−6488.
(32) Shenoy, S. L.; Fujiwara, T.; Wynne, K. J. *Macromolecules* **2003**, *36*, 3380−3385.
(33) Bonavoglia, B.; Storti, G.; Morbidelli, M. *Ind. Eng. Chem. Res.* **2006**, *45*, 1183−1200.
(34) Peng, D. Y.; Robinson, D. B. *Ind. Eng. Chem. Fundam.* **1976**, *15*, 59−64.
(35) Poling, B. E.; Prausnitz, J. M.; O'Connell, J. P. *The Properties of Gases and Liquids*, 5th ed.; McGraw-Hill Higher Education: Columbus, OH, 2001; p A.6.
(36) Wenzel, J. E.; Lanterman, H. B.; Lee, S. *J. Chem. Eng. Data* **2005**, *50*, 774−776.
(37) Crank, J. *The Mathematics of Diffusion*, 2nd ed.; Clarendon Press: Oxford, U.K., 1975; pp 90−96.
(38) Fiaconnèche, B.; Martin, J.; Klopffer, M. H. *Oil Gas Sci Technol.* **2001**, *56*, 261−278.
(39) Michaels, A. S.; Parker, R. B. *J. Polym. Sci.* **1959**, *41*, 53−71.
(40) Barton, A. F. M. *CRC Handbook of Solubility Parameters and Other Cohesion Parameters*, 2nd ed.; CRC Press: Boca Raton, FL, 1991.
(41) Sanchez, I. C.; Lacombe, R. H. *Macromolecules* **1978**, *11*, 1145−1156.
(42) McHugh, M. A.; Krukonis, V. J. *Supercritical Fluid Extraction: Principles and Practice*, 2nd ed.; Butterworth Heinemann: Boston, 1994.
(43) Rodgers, P. A. *J. Appl. Polym. Sci.* **1993**, *50*, 2075−2083.
(44) Kennedy, K. A.; DeSimone, J. M.; Roberts, G. W. *J. Polym. Sci., Part B: Polym. Phys.* **2002**, *40*, 602−604.
(45) Ahmed, T. S.; DeSimone, J. M.; Roberts, G. W. *Chem. Eng. Sci.* **2004**, *59*, 5139−5144.
(46) Giaconia, A.; Filardo, G.; Scialdone, O.; Galia, A. *J. Polym. Sci., Part A: Polym. Chem.* **2006**, *44*, 4122−4135.

MA702087S